2010 IEEE International Conference on Robotics and Automation
Anchorage Convention District
May 3-8, 2010, Anchorage, Alaska, USA

Integrated Silicon-PDMS Process for Microrobot Mechanisms

Aaron P. Gerratt, Ivan Penskiy, and Sarah Bergbreiter

Abstract— **The first MEMS process integrating soft elastomers in a standard silicon-on-insulator (SOI) wafer without assembly has been demonstrated for use in microrobotic mechanisms. This process allows silicon and poly(dimethylsiloxane) (PDMS) features to be defined in-plane with feature sizes down to 2 μm. Test structures have been used to characterize the Young's modulus of the resulting PDMS at 1.4 MPa along with adhesion to silicon structures. In addition, compliant flexures have been designed, fabricated and characterized for eventual use in microrobot legs. Test structures have been mechanically folded 180° out of plane over 60 times without failure.**

I. INTRODUCTION

Attention to microrobots has grown dramatically in the past decade. Previous works include walking robots [1], [2], flying robots [3], [4], and crawling robots [5]. As the number of different mobility methods and mechanism complexity increases, microfabrication techniques have also had to evolve and be developed to support the complex requirements of these microrobots. Ebefors demonstrated polyimide thermal actuators as part of one of the first millimeter-scale walking microrobots [1]. Hollar's 10 mg silicon microrobot was built using traditional silicon microelectromechanical systems (MEMS) processing to include thick structural layers for high force actuators and thin polysilicon hinges for multi-DOF robot legs [2]. Wood developed the Smart Composite Microstructures (SCM) process by combining laser micromachined carbon fiber with polymer films to build millimeter sized compliant mechanisms for a 60 mg robotic insect [6]. To create thin, compliant wings for micro air vehicles, Tanaka combined MEMS deep reactive ion etching for mold building with parylene and polyurethane [3].

Each of these processes offers advantages and drawbacks for fabricating large numbers of millimeter-scale autonomous microrobots. An ideal fabrication process would be simple, fast, robust, provide for batch processing and small feature sizes, as well as integration with efficient microactuators. Hollar's process provides small feature sizes, batch processing and integration with MEMS electrostatic actuators, but lacks robustness and is both complex and time-consuming [2]. Ebefors created small features and demonstrated robustness by adding polyimide to silicon, but the robot was based on highly inefficient actuators [1]. The SCM process requires folding of laser-cut carbon fiber sheets which results in serial processing and larger feature sizes [6]. However, robots made in this process are generally more robust than their MEMS counterparts.

While MEMS processes generally provide for small feature sizes, batch processing and good integration with microactuators, a primary drawback of MEMS processes for microrobot fabrication is the materials generally used. Traditional MEMS devices include semiconductors, metals and dielectrics with Young's moduli on the order of GPas. These materials result in stiff, often brittle microrobots that are limited in their mobility methods. Recent work by Bergbreiter integrated soft elastomers such as poly(dimethylsiloxane) (PDMS) into MEMS processes for the first time in microrobotics [7]. PDMS has a Young's modulus on the order of a single MPa and was demonstrated for use in an energy storage and quick-release mechanism for a jumping microrobot. These devices, however, require separate fabrication and assembly of the silicon and elastomer components, which greatly increases the necessary fabrication time, decreases the device yield, and can only be used to fabricate relatively large features in the elastomer (approximately 100 μm).

The process presented in this paper integrates PDMS and silicon for the first time in a simple MEMS batch fabricated process. The soft elastomer increases the robot robustness and allows for the fabrication of complex mechanisms such as energy storage/quick release structures and legs that can be folded out of plane. Other than folding of structures, no post-process assembly is required and small feature sizes of 2 μm can be achieved in both the silicon and the elastomer. In addition, the presented fabrication process will ultimately improve other MEMS devices such as electrostatic inchworm motors [8] and energy storage devices [7]. The ultimate goal of this research is to develop a processing toolbox for autonomous millimeter-scale robots.

Section II describes the fabrication process used to create the microrobot mechanisms, and the process is characterized in Section III. The design of components for microrobots is discussed in Section IV, with results from fabricated mechanisms presented in Section V.

II. MICROFABRICATION OF INTEGRATED SILICON/PDMS MECHANISMS

The primary innovation in this paper is the integrated silicon-PDMS process for the fabrication of microrobot mechanisms (Figure 1). The process is very similar to the commercially available SOI-MUMPS® process with the addition of an extra mask step to define the PDMS features [9]. While the focus of this paper is on fabrication with Sylgard® 184 PDMS, the process has also been used with

S. Bergbreiter is in the Mechanical Engineering Department and the Institute for Systems Research, University of Maryland, College Park, USA sarahb@umd.edu
A. Gerratt and I. Penskiy are in the Department of Mechanical Engineering, University of Maryland, College Park, USA gerratt,ipenskiy@umd.edu

978-1-4244-5040-4/10/$26.00 ©2010 IEEE

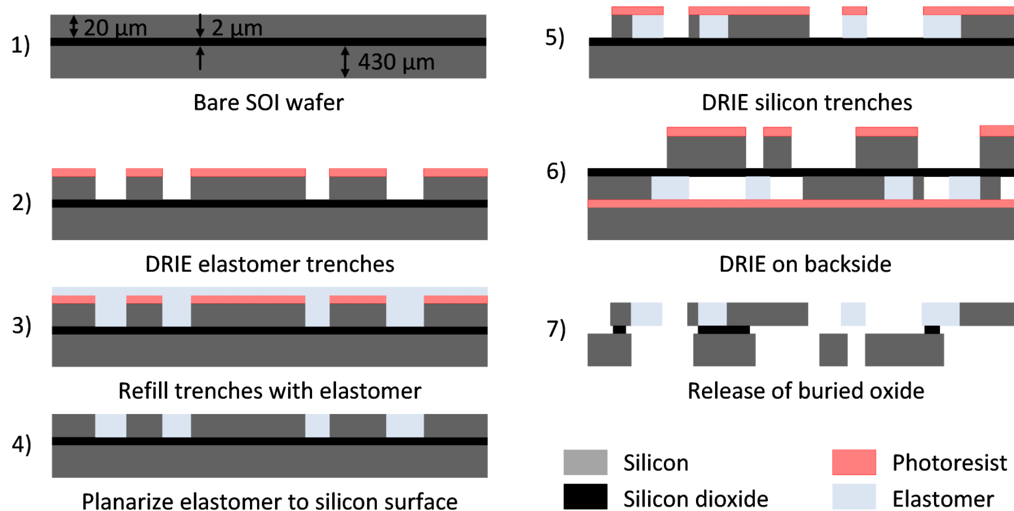

Fig. 1. Microfabrication Process

Sylgard® 186 PDMS and Dragon Skin® from Smooth-On, and can likely be used with many other addition cure polymers or room temperature vulcanizing rubbers. Devices were all fabricated on a silicon-on-insulator (SOI) wafer (500 μm handle layer thickness, either 2 or 4 μm buried oxide (BOX) layer thickness, and 20 μm device layer thickness).

In step 2, photoresist was patterned on the device layer and a deep reactive ion etch (DRIE) was performed down to the buried oxide. An oxygen plasma clean was performed in order to remove any residual passivation layer remaining from the DRIE.

Sylgard® 184 PDMS from Dow Corning was mixed in a 10:1 ratio of base to curing agent and degassed in vacuum at 1 Torr for 15 minutes. The PDMS was then spread across the wafer in step 3, with the photoresist still on the surface of the wafer. The PDMS coated wafer was then degassed to remove any air bubbles from the PDMS and to ensure that the trenches etched in the wafer were completely refilled with PDMS. For feature sizes down to 2 μm (for an aspect ratio of 10:1), 10 minutes at 1 Torr was found to be sufficient to ensure complete refill of the trenches. Excess PDMS was removed by spinning the wafer at 2000 RPM for 120 seconds. The wafer was then degassed for another 10 minutes at 1 Torr to ensure no air bubbles were introduced during the spinning process. The PDMS was cured in an oven at 80°C for 2 hours.

To allow for a second lithography step to be performed, the PDMS was removed from the surface of the wafer in step 4. This was accomplished by using a razor blade as a squeegee to scrape the wafer surface. This process removes the majority of the PDMS and resist. The remaining photoresist was used to liftoff any residual PDMS. The liftoff leaves small particles of PDMS on the surface of the wafer, so a brief soak in a n-methylpyrrolidone (NMP) and tetrabutylammonium fluoride (TBAF) in a 3:1 ratio was performed. This solution is a commonly used PDMS wet etchant [10] and removes any residual PDMS pieces that remain on the surface of the wafer.

In step 5, photoresist was again patterned on the device layer of the wafer and another DRIE was performed down to the buried oxide, patterning silicon features around the elastomer features. Exposed PDMS showed good resistance to the DRIE, as it was etched only on the order of nanometers. A layer of photoresist was then spun on the top of the wafer to protect it during later processing steps.

The backside of the wafer was also patterned to allow structures to freely move without sticking to the wafer surface. In step 6, photoresist was patterned on the backside of the wafer, and afterwards the device layer of the wafer was bonded with a thin layer of photoresist to a handle wafer. A DRIE was performed on the backside of the SOI wafer down to the buried oxide. After the DRIE, a solvent release was used to separate the SOI wafer from the handle wafer. Finally in step 7, a 6:1 buffered hydrofluoric acid (BHF) etch of the buried oxide was used to release some of the silicon and PDMS features. For this, alternating dips in BHF and deionized (DI) water were performed to ensure the survival of the PDMS in the BHF. Extended soaks of PDMS in BHF etches and deteriorates the PDMS [11], but intermittent soaks in DI water proved to extend the period over which the PDMS could be immersed in BHF and still survive. Soaking in 6:1 BHF for 20 minutes and then soaking in DI for 5 minutes was sufficient to limiting the etching of the PDMS.

Overall, this process has proved to be extremely repeatable. The yield for devices that utilize small features is almost 100%. As the width of the PDMS traces gets wider, device yield decreases. Features hundreds of microns wide have been fabricated, but not reliably.

III. PROCESS CHARACTERIZATION

To better use this process in microrobotic mechanisms, the mechanical properties of the PDMS after processing have been characterized. The process defined in Section II has the

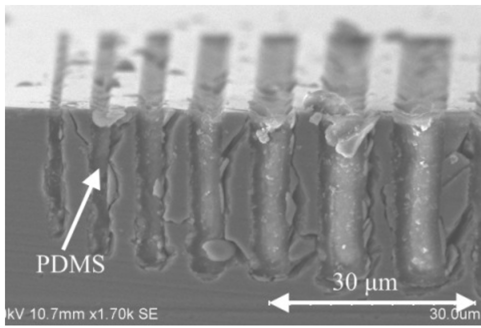

Fig. 2. Trenches etched in silicon that have been refilled with PDMS

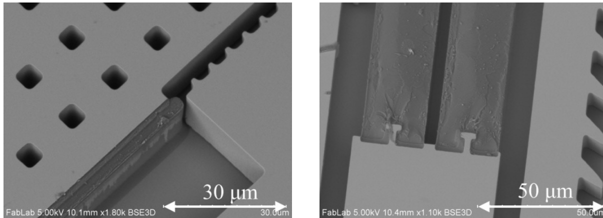

Fig. 3. Small and large PDMS features have been fabricated in contact with silicon features

benefit of great versatility compared to previous work using post-process assembly, so features of any 2D geometry can be fabricated. PDMS feature sizes from 3 μm up to 100s of μm have been demonstrated, shown in Figure 3. Length of the features, however, is not an issue, as traces many millimeters in length have been repeatedly fabricated.

Highly dense PDMS features do not fabricate as well as spaced features. Traces that are 30 μm in width but separated by only 10 μm will have a smaller yield than 30 μm features that are separated by 100 μm. This is due to a thinning of the photoresist around elastomer features because of any changes in the topography at the surface of the wafer after step 4 of the fabrication process. Failure occurs when the photoresist is thinned so much that it is etched through during the DRIE in step 5. This issue could be eliminated with a thicker mask layer or a different mask layer with higher selectivity to silicon. High aspect ratio features have also been repeatedly fabricated, as shown in Figure 2. Etched trenches with an aspect ratio of about 60:1 have been successfully refilled.

A. Adhesion Between Silicon and PDMS

One of the primary issues still to be addressed in this process is robust adhesion between the PDMS and silicon. While large strains can be achieved, the failure of most devices comes from delamination of the PDMS from the silicon rather than the PDMS reaching its failure strain. One cause is the slight etching of PDMS during the release process. Figure 4 shows a PDMS feature before and after the release process. It is evident that the interface between the silicon and PDMS has been etched, which leads to delamination of the PDMS from the silicon under high strains.

To better quantify the adhesion of the silicon and PDMS, the features in Figures 5 and 6 were fabricated. The device in Figure 5 was used to determine the silicon/PDMS adhesion when the forces are primarily normal. The device in Figure 6 was used to determine the silicon/PDMS adhesion when the forces are primarily shear. Under normal loads, the ultimate pressure at which PDMS delaminated from the silicon varied from device to device, but always at pressures in excess of 0.8 MPa and was as high as 1.6 MPa. Under shear loads, the PDMS delaminated from the silicon between 40 and 70 kPa. The difference between the shear and normal pressures is quite dramatic and the mechanism for the difference is still being investigated. It is interesting to note that under shear loads, the forces seen at the silicon/PDMS interface were not completely shear. Delamination typically occurred when the cross section of the elastomer shrank as the PDMS elongated, so the effective load at the interface was a combination of both normal and shear forces.

Adhesion between silicon and PDMS also changes over time. While no quantified data is currently available, it has been repeatedly observed that the silicon/PDMS adhesion improves after sitting in a dry box for several days. The extent of the improvement and the mechanism causing this is still being investigated. All of the data presented in this paper was from devices that were fabricated and tested in a 72 hour period.

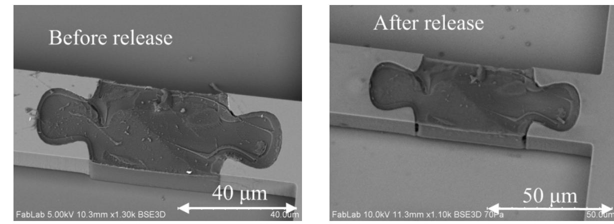

Fig. 4. A PDMS features before and after the release process in BHF

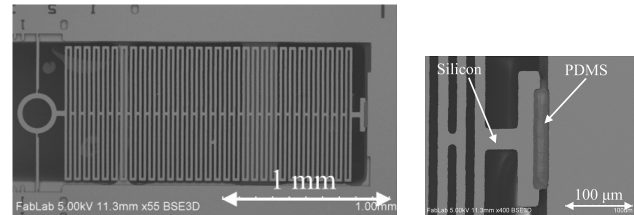

Fig. 5. SEM images of the feature used to measure the force required for delamination due to normal forces

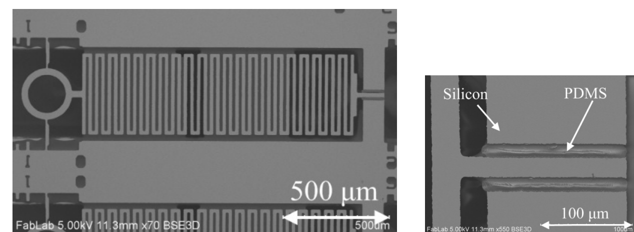

Fig. 6. SEM images of the feature used to measure the force required for delamination due to shear forces

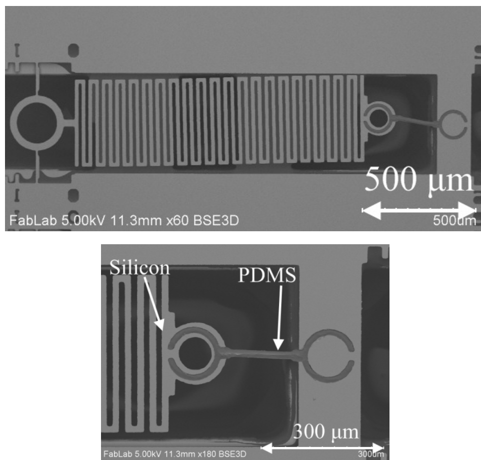

Fig. 7. SEM image of the feature used to measure stress-strain and the Young's Modulus

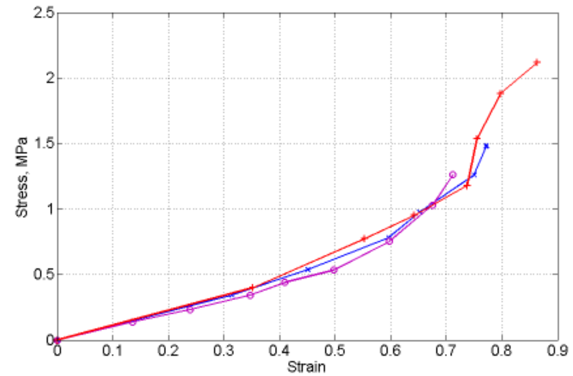

Fig. 8. Stress-strain diagram for devices shown in Figure 7. 3 trials out of 12 are plotted.

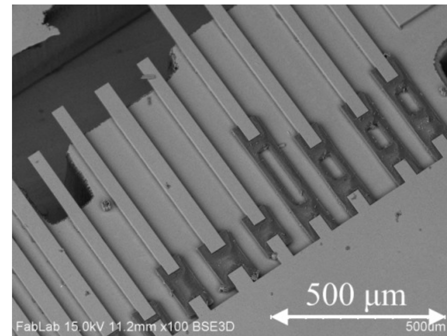

Fig. 9. SEM image of fabricated PDMS compliant hinges

B. Stress-Strain and Ultimate Strain Behavior of PDMS

Other mechanical properties of the system that were measured were stress and strain, the Young's modulus, and the ultimate failure strain. The device in Figure 7 was used to determine all of these properties. A PDMS spring was fixed to an anchor at one end and to a serpentine spring at the other end. A probe was used to stretch the serpentine spring which applied the same force on the PDMS spring. The spring constant of the serpentine spring was designed to be approximately 4.5 N/m using ANSYS. This spring constant combined with the elongation of the silicon spring was used to determine the load on the PDMS.

Figure 8 shows a stress-strain curve for one of these devices. The cross-sectional area (15 μm x 20 μm) of the spring was used to calculate stress and the Young's modulus. For the post-fabrication PDMS springs, the modulus was calculated at 1.4 MPa in the linear interval of the stress-strain curve. This is in relatively close agreement to the Young's modulus for un-processed macro-scale PDMS features reported in [12] of 1.8 MPa, although this number is artificially high since it incorporates points where the strain is non-linear. The stress-strain curve for PDMS also exhibits strain-toughening, where the Young's modulus increases with strain, as can be seen in Figure 8. While straining of bulk PDMS in excess of 200% or 300% is commonly reported [7], [12], typically a maximum strain of about 90% was reached before delamination. Similar structures have demonstrated strains up to 200%, so increased elongation is possible if the silicon/PDMS adhesion can be improved.

IV. MECHANISM DESIGN

A. Compliant Hinges

One of the significant limitations on current MEMS processing techniques is that they are almost all exclusively two dimensional, and it is difficult to assemble three dimensional structures after fabrication is complete. Three dimensional processes exist, but are not widely used and often require serial fabrication, not parallel fabrication, which increases fabrication time and costs [13] . The microrobot described in [14] used polysilicon rods and staples to create hinges for its legs. One of the drawbacks of this design was that the fabrication process was relatively complex and the failure rate of the hinges was high. Using the fabrication process from Section II, polymer hinges for in-plane and out-of-plane flexure were designed, as shown in Figure 9.

The hinges in Figure 9 function as simple PDMS cantilevers, but the high strains and low Young's modulus of this material allow for large angular deflections. In addition, future hinge designs can take advantage of better normal adhesion or more complex designs such as the anti-buckling hinge shown in [6].

B. Future Robot Legs

Given an established process for fabrication of PDMS hinges, legs for microrobotic systems become more feasible. The baseline features shown here can easily be scaled to create legs for a robotic system, such as that shown in Figure 10. This system contains three links. The small top link is fixed in place. The longest link is the leg itself, which is connected end-to-end with the fixed leg. The leg is driven with a third link which is connected to the center of the leg with another PDMS joint. The driving link could be integrated with the shuttle of an inchworm motor, such as that presented in [15]. ANSYS was used to calculate the force as a function (Figure 11) of the rotation angle of a hinge similar

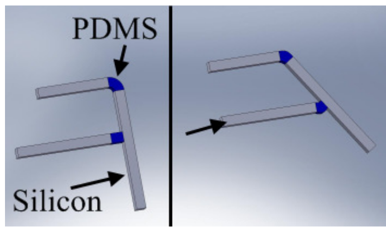

Fig. 10. Drawing of a possible robot leg with elastomer joints

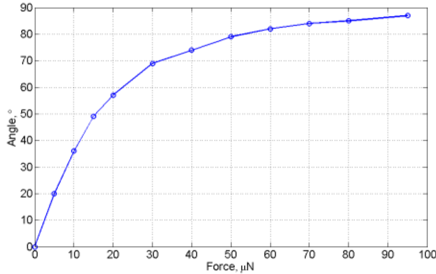

Fig. 11. Force as a function of rotation angle to rotate a hinge such as the ones shown in Figure 9

to that at the end-to-end joint shown in Figure 10. The force required to rotate 87° was about 100μN, which could easily be generated by an electrostatic gap-closing inchworm motor.

For some instances, however, a thin leg such as that shown in Figure 10 is not sufficient to withstand the forces or payload the robot would be subjected to. In this case, more robust links could be fabricated, such as that shown in Figure 12. The feature would be fabricated in plane, released from the substrate, and then assembled out of plane, much like the SCM process. To hold the features together, an oxygen plasma treatment would be used to bond the two PDMS tabs, as is often done in microfluidics [16] or silicon snap-locks could be used as shown in [17]. This type of structure could be used not only for legs, but also as a shell for a microrobotic system.

V. INITIAL RESULTS

The compliant elastomer joints that were designed preformed well as hinges. As can be seen in Figure 13, the

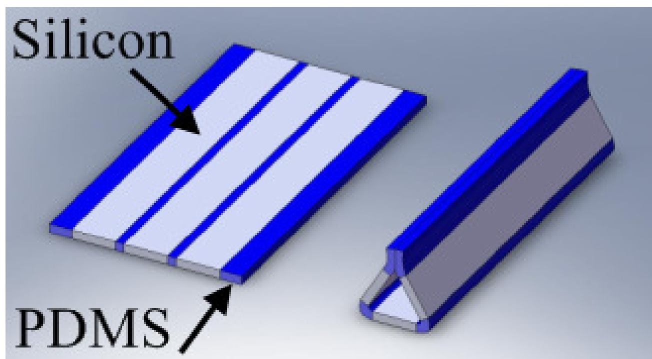

Fig. 12. Drawing of a folded feature before and after assembly

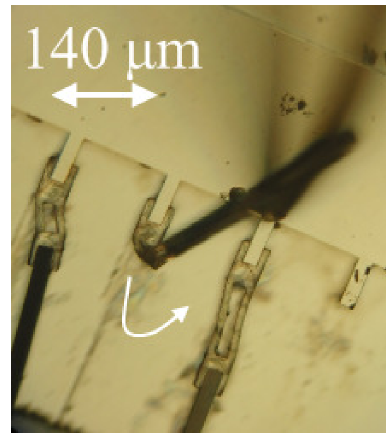

Fig. 13. A hinge, similar to that in Figure 9, that has been rotated 180° out of plane with a probe

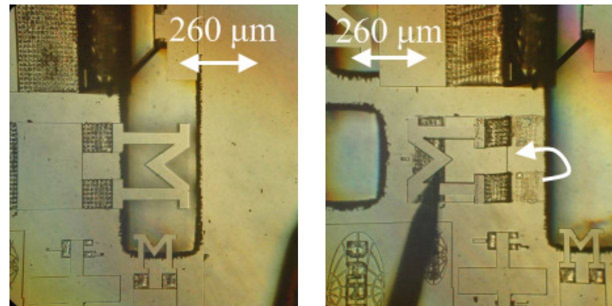

Fig. 14. A silicon “M” with PDMS hinge before and after being manually flipped 180 degrees with a probe

hinges can be manipulated in any direction. The hinge shown in Figure 13 was rotated in-plane 90° over 100 times without failure. Even when stressed, the hinge performed well and snapped back into position when released. The “M” shown in Figure 14 was flexed 180 degrees out of plane 60 times without failure. Hinges were also used in the feature shown in Figure 15. After fabrication was complete, a probe was used to manipulate the silicon frame and PDMS hinge to hold the system more rigidly out of plane.

Some of the hinges designed in this initial phase suffered due to lengths that were only a few times longer than they were tall. These hinges preferred to bend where it met the silicon, as can be seen in Figure 14, as opposed to bending consistently through the length of the hinge as was expected. The hinges can be made to be more compliant through one of three methods. Using an SOI wafer with a thinner device layer or increasing the length of the spring while holding the height constant would increase ratio of length to height of the hinge and will make them more compliant in the out-of-plane direction. Voids could also be introduced into the design of the elastomer hinges to make them more compliant, such as in the hinges shown in Figure 9. The PDMS hinge in Figure 14 had 5 μm holes at 15 μm spacings that provided a little additional compliance in the hinges, but larger or more dense holes would likely prove beneficial.

VI. CONCLUSIONS AND FUTURE WORKS

A. Conclusions

The first MEMS process incorporating silicon and PDMS that does not require post-process assembly has been demonstrated. PDMS features can range from small 3 μm wide traces to large geometries 100s of microns in size. The mechanical properties of the post-processed PDMS was explored and showed a Young's modulus of about 1.4 MPa. The PDMS also showed good adhesion when normal forces were applied, but poor adhesion when shear forces were applied. The process was used to fabricate robust compliant hinges that could be cycled many times without failure. Mechanisms utilizing these hinges could easily be applied in the design of legs for microrobots.

B. Future Works

The fabrication process and mechanisms described in this paper outline the processing groundwork required to develop microrobots with silicon and PDMS components. The process needs to be further developed in order to achieve higher strains before delamination of the PDMS from the silicon, and a number of mechanical and chemical methods are being pursued. Methods being explored include mechanical interlocking silicon and PDMS features and applying chemical adhesion promoters prior to application of the PDMS. In addition, initial process characterization results are now being used to design and fabricate the legs and mechanisms required for a mobile microrobot, though lifetime tests and fatigue of the PDMS must be examined.

Future work will include the implementation of this process to increase friction for improved efficiency and force density in electrostatic inchworm motors, which have already been integrated in the actuation system for jumping microrobots [15]. The PDMS in this process can be used in an energy storage system to quickly release stored mechanical energy for a jump in these robots. PDMS features can also be integrated into the design of silicon mechanisms to make them more robust. Much like the skin on a person, thin layers of PDMS could be used to protect mechanical and electrical components in microrobotic systems, as in [18].

VII. ACKNOWLEDGMENTS

This work is supported by a DARPA Young Faculty Award. The authors gratefully acknowledge the support of the Maryland NanoCenter and its FabLab.

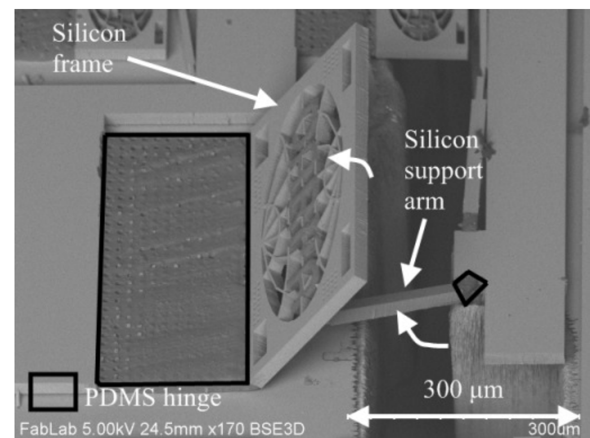

Fig. 15. A silicon frame was fabricated in plane, rotated on a hinge out of plane, and kept out of plane with another silicon piece positioned with a probe

REFERENCES

[1] T. Ebefors, J. U. Mattsson, E. Kalvesten, and G. Stemme, "A walking silicon microrobot," in *Transducers 1999*, Sendai, Japan, 1999, pp. 1202–1205.

[2] S. Hollar, S. Bergbreiter, and K. S. J. Pister, "Bidirectional inchworm motors and two-DOF robot leg operation," in *Transducers 2003*, Boston, MA, 2003, pp. 262–267.

[3] H. Tanaka, K. Matsumoto, and I. Shimoyama, "Design and performance of micromolded plastic butterfly wings on butterfly ornithopter," in *IROS 2008*, Nice, France, 2008, pp. 3095–3100.

[4] R. J. Wood, "The first takeoff of a biologically inspired at-scale robotic insect," *IEEE Transactions on Robotics*, vol. 24, no. 2, pp. 341–347, 2008.

[5] B. R. Donald, C. G. Levey, C. D. McGray, I. Paprotny, and D. Rus, "An untethered, electrostatic, globally controllable MEMS microrobot," *Journal of Microelectromechanical Systems*, vol. 15, no. 1, pp. 1–15, 2006.

[6] R. J. Wood, S. Avadhanula, M. Menon, and R. S. Fearing, "Microrobotics using composite materials: the micromechanical flying insect thorax," in *IEEE Inernational Conference on Robotics and Automation*, Taipei, Taiwan, 2003.

[7] S. Bergbreiter and K. S. J. Pister, "An elastomer-based micromechanical energy storage system," in *ASME International Mechanical Engineering Congress and Exposition*, Chicago, IL, 2006.

[8] R. Yeh, S. Hollar, and K. S. J. Pister, "Single mask, large force, and large displacement electrostatic linear inchworm motors," *Microelectromechanical Systems, Journal of*, vol. 11, no. 4, pp. 330–336, 2002.

[9] "SOIMUMPS," 2008. [Online]. Available: http://www.memscap.com/

[10] B. Balakrisnan, S. Patil, and E. Smela, "Patterning PDMS using a combination of wet and dry etching," *Journal of Micromechanics and Microengineering*, vol. 19, no. 4, p. 047002 (7pp), 2009.

[11] J. Garra, T. Long, J. Currie, T. Schneider, R. White, and M. Paranjape, "Dry etching of polydimethylsiloxane for microfluidic systems," *Journal of Vacuum Science and Technology A*, vol. 20, no. 3, pp. 975–982, 2002.

[12] F. Schneider, T. Fellner, J. Wilde, and U. Wallrabe, "Mechanical properties of silicones for MEMS," *Journal of Micromechanics and Microengineering*, vol. 18, no. 6, 2008.

[13] A. Bertsch, S. Jiguet, and P. Renaud, "Microfabrication of ceramic components by microstereolithography," *Journal of Micromechanics and Microengineering*, vol. 14, no. 2, pp. 197—203, 2004.

[14] S. Hollar, A. M. Flynn, S. Bergbreiter, and K. S. J. Pister, "Robot leg motion in a Planarized-SOI, Two-Layer Poly-Si process," *Journal of Microelectromechanical Systems*, vol. 14, no. 4, pp. 725–740, 2005.

[15] S. Bergbreiter and K. S. J. Pister, "Design of an autonomous jumping microrobot," in *IEEE International Conference on Robotics and Automation*, Roma, Italy, Apr. 2007, pp. 447–453.

[16] D. C. Duffy, J. C. McDonald, J. A. Schueller, and G. M. Whitesides, "Rapid prototyping of microfluidic systems in poly(dimethylsiloxane)," *Analytical Chemistry*, vol. 70, pp. 4974–4984, 1998.

[17] R. Yeh and K. S. J. Pister, "Design of Low-Power silicon articulated microrobots," *Journal of Micromechatronics*, vol. 1, no. 3, pp. 191–203, 2001.

[18] J. M. Han, J. W. Han, J. Y. Chun, C. H. Ok, and D. S. Seo, "Novel encapsulation method for flexible organic Light-Emitting diodes using poly (dimethylsiloxane)," *Japanese Journal of Applied Physics*, vol. 47, no. 12, pp. 8986–8988, 2008.